

Dynamics and cluster formation in charged and uncharged Ficoll70 solutions

Swomitra Palit and , and Anand Yethiraj

Citation: [The Journal of Chemical Physics](#) **147**, 074901 (2017); doi: 10.1063/1.4986366

View online: <http://dx.doi.org/10.1063/1.4986366>

View Table of Contents: <http://aip.scitation.org/toc/jcp/147/7>

Published by the [American Institute of Physics](#)

**COMPLETELY
REDESIGNED!**

A graphic element consisting of two square icons. The left icon contains a line graph with a single wavy line. The right icon contains a grid of small circles.

PHYSICS
TODAY

Physics Today Buyer's Guide
Search with a purpose.

Dynamics and cluster formation in charged and uncharged Ficoll70 solutions

Swomitra Palit^{a)} and Anand Yethiraj^{b)}

*Department of Physics and Physical Oceanography, Memorial University, St. John's,
Newfoundland and Labrador A1B3X7, Canada*

(Received 4 June 2017; accepted 1 August 2017; published online 15 August 2017)

We apply pulsed-field-gradient NMR (PFG NMR) technique to measure the translational diffusion for both uncharged and charged polysaccharide (Ficoll70) in water. Analysis of the data indicates that the NMR signal attenuation above a certain packing fraction can be adequately fitted with a bi-exponential function. The self-diffusion measurements also show that the Ficoll70, an often-used compact, spherical polysucrose molecule, is itself nonideal, exhibiting signs of both softness and attractive interactions in the form of a stable suspension consisting of monomers and clusters. Further, we can quantify the fraction of monomers and clusters. This work strengthens the picture of the existence of a bound water layer within and around a porous Ficoll70 particle. *Published by AIP Publishing.* [<http://dx.doi.org/10.1063/1.4986366>]

I. INTRODUCTION

A highly branched copolymer of two short building blocks, sucrose and epichlorohydrin, Ficoll70 has been widely used in studies of macromolecular crowding and for applications in blood preservation and renal filtration due to its high hydrophobicity as well as its charge neutral globular form.^{1–12} This synthetic carbohydrate polymer has been used by many investigators to produce a resemblance of the high total concentrations that are encountered in the cytoplasm.¹³

While some experiments found that the diffusion of Ficoll70 fits the accepted model for the diffusion of a hard sphere through cylindrical pores,^{14,15} other experiments found that either Ficoll70 is more spherical and protein-like than dextran¹⁶ or it is more deformable than globular proteins.¹⁷ Based on experiments *in vivo*, Asgeirsson *et al.* conjectured that Ficoll70 is sufficiently crosslinked such that it cannot reptate but is not a rigid sphere.¹⁸ Fissell and collaborators measured the transport of Ficoll70 through silicon slit nanopore membranes. They observed that Ficoll70 molecules could penetrate the pore even when the Stokes-Einstein radius was greater than the slit width, implying deformability. They surmised that the Ficoll70 molecule is not spherical, is not rigid, or exhibits a different conformation in ionic solutions.⁵

The most advanced analysis of Ficoll70 solution properties has been done in the renal filtration literature.^{4–6,19–22} Fissell *et al.* used standard multidetector size-exclusion chromatography (SEC) on Ficoll to show that the Mark-Houwink exponents for the molecular mass dependence of the intrinsic viscosity were 0.34 (Ficoll70) and 0.36 (Ficoll400), between the value of 0 for a solid sphere and 0.5–0.8 for

a random coil.²³ Their result agrees closely with those of Lavrenko *et al.*²⁴ Groszek *et al.* used similar experiments to demonstrate that charged Ficoll70 was significantly retarded compared with uncharged Ficoll70 across the rat glomerular filtration barrier.⁴ Georgalis *et al.* found two different sizes of particles in Ficoll70 by means of light scattering experiments.²⁵

In this study, we employ pulsed-field-gradient (PFG) NMR to monitor the self-diffusivities of uncharged and charged Ficoll70 in deionized water. Because of the spectral selectivity of NMR, we can simultaneously (see Fig. 1) obtain signal from both the Ficoll70 and water species. In a companion work, we focus on polymer structure and dynamics²⁶ in the presence of Ficoll70 crowder. Ficoll is an often-used crowder. In the understanding of macromolecular crowding, it is important to understand well the properties of the crowder. In this work, we examine the properties of both charged and uncharged Ficoll70 for evidence of cluster formation in equilibrium, a phenomenon, distinct from bulk phase separation, that has been identified in colloids and proteins where short-ranged attractions coexist with longer-ranged (typically electrostatic) repulsive interactions.^{27–32}

II. MATERIALS AND METHODS

Ficoll®PM 70 (referred to as Ficoll70 in the text) with average molecular weight of 70 000 [mean radius (R_c) 4.5–5.5 nm^{8,25,33–35}] was purchased from Sigma Aldrich and used without further purification. In this work, we use the value of $R_c = 4.6$ nm.³⁴ Charged Ficoll70 (Ficoll CM 70) was a carboxymethylated derivative of Ficoll PM70, made as described in Ref. 4. It was a gift from Fissell and was used as received after having been neutralized and dialyzed against distilled water for 4 days. Experimental packing fractions (Φ_F) of Ficoll70 were calculated using the partial specific volume of Ficoll70, $\bar{v} = 0.67 \text{ cm}^3/\text{g}$ ¹⁰ and are defined as

^{a)}Electronic mail: swomitra@mun.ca

^{b)}Electronic mail: ayethiraj@mun.ca

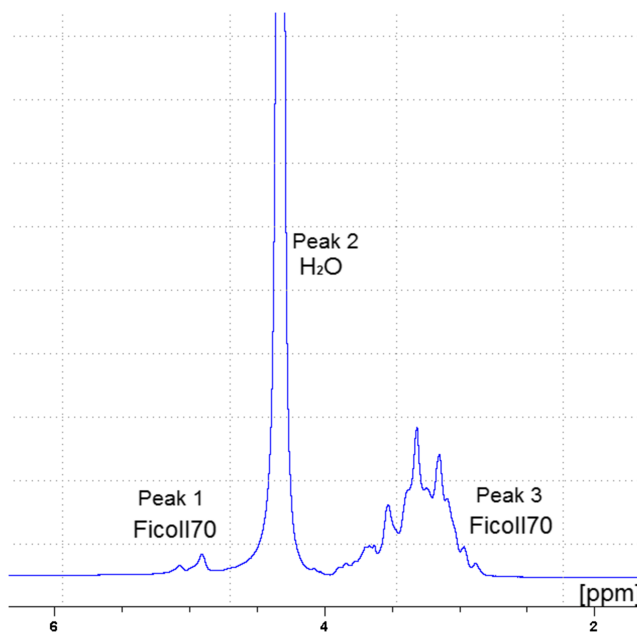


FIG. 1. 1D ^1H -NMR spectrum for Ficoll70/ H_2O sample at a sample temperature 298 K.

$$\Phi_F = \left(\frac{M_{\text{Ficoll}} \times 0.67}{M_{\text{Ficoll}} \times 0.67 + V_{\text{H}_2\text{O}}} \right). \quad (1)$$

Here M_{Ficoll} and $V_{\text{H}_2\text{O}}$ are the mass of Ficoll70 in units of gram and volume of water in units of cm^3 , respectively.

For sample preparation, the desired packing fraction of Ficoll70 was dissolved in deionized H_2O . For charged Ficoll70 solutions, the conductivity was controlled, using KCl, to a value of ≈ 1 mS/cm (see Table I) in order to ensure a consistent Debye-Hückel screening length ($\kappa R_c \sim 1.4$) for all samples. The solution was stirred for 10 h. Samples were then transferred to 5 mm outer diameter NMR tubes.

A. PFG NMR

The one-dimensional 1D proton NMR spectrum has been observed for different species in all samples at a resonance frequency of 600 MHz on a Bruker Avance II spectrometer. Figure 1 shows well-separated peak regions related to this system. Peak 1 and Peak 3 are the Ficoll70 peaks whereas Peak 2 is for H_2O molecules in solution. All NMR experiments were performed at $T = 298$ K. The self-diffusion measurements were carried out in a diffusion probe Diff 30

TABLE I. Comparison of the zeta potential for charged and uncharged Ficoll70.

Species	Zeta potential (mV)	Mobility ($\mu\text{m cm V/s}$)	Conductivity (mS/cm)
Charged Ficoll70 (without salt)	-27 ± 4	-1.4 ± 0.2	0.1 ± 0.02
Charged Ficoll70 (salt added)	-29 ± 2	-1.3 ± 0.4	1.1 ± 0.01
Uncharged Ficoll70	-5.2 ± 0.2	-0.4 ± 0.02	0.04 ± 0.01

and with maximum field gradient 1800 G/cm (18 T/m). Diffusion was measured with a pulsed-field-gradient stimulated echo sequence with trapezoidal gradient pulses.³⁶ The diffusion coefficient of a molecule in an aqueous solution is obtained from the attenuation of the signal according to the equation

$$S(k) = S(0) \exp(-Dk), \quad (2)$$

where $S(k)$ is the intensity of the signal in the presence of field gradient pulse, $S(0)$ is the intensity of the signal in the absence of the field gradient pulse, $k = (\gamma\delta g)^2(\Delta - \delta/3)$, $\gamma = \gamma^{\text{H}} = 2.657 \times 10^8 \text{ T}^{-1}\cdot\text{s}^{-1}$ is the proton gyromagnetic ratio, $\delta = 2$ ms is the duration of field gradient pulse, $\Delta = 100$ ms is the time period between two field gradient pulses, and g is the amplitude of field gradient pulse.

B. Zeta potential

The zeta potential (ζ) and electrophoretic mobility of Ficoll70 solutions, shown in Table I, were measured by a Zetasizer Nano Z system (Malvern Instruments Ltd., Malvern, United Kingdom). The dimensionless zeta potential $\Psi = \zeta e/k_B T = 1.1 \pm 0.2$ and 0.21 ± 0.02 for charged and uncharged Ficoll70, respectively. The solutions of charged Ficoll70 were all prepared with added salt in order to keep the conductivity at 1 mS/cm, resulting in a Debye-Hückel screening length $\kappa^{-1} = 3.2 \pm 0.5$ nm. This corresponds to a $\kappa R_c \sim 1.4$. Given the value of the dimensionless zeta potential Ψ and κR_c , i.e., both of order unity, electrostatics should clearly be important, but not overwhelmingly so.

C. Bulk viscosity measurement

Experiments were performed on an Anton Paar Physica MCR 301 rheometer, where the cone-plate measuring system was used to extract the flow curves. The cone-plate geometry has a diameter of 50 mm and a cone angle of 0.5° . All samples were pre-sheared for 1 min before collecting data. The flow curves experiments were carried out with the shear rate varying from 0.001 to 100 s^{-1} . For all samples reported in this work, viscosity remains constant as the shear rate is varied.

III. DIFFUSION MODEL

The PFG NMR signal attenuation of Ficoll70 shows a monoexponential decay with the gradient strength parameter at a low packing fraction [$\Phi_F < 0.05$ (uncharged) and $\Phi_F < 0.1$ (charged)]. This implies either that it is a single component system or that there are multiple components (e.g. a monomer and cluster) that exchange very rapidly between the monomer and aggregate on the time scale of the NMR experiment.³⁷ Given the larger size of Ficoll70, the diffusion time of the monomer $\sim 1 \mu\text{s}$; thus residence times of the Ficoll70 molecule within clusters will be a few micro-seconds or longer. Hence the fact that the signal attenuation associated with the Ficoll70 peak exhibits monoexponential behaviour [Fig. 2(a)] at low packing fractions suggests that the exchange between Ficoll70 clusters and monomers must be very rapid on the NMR time scale.

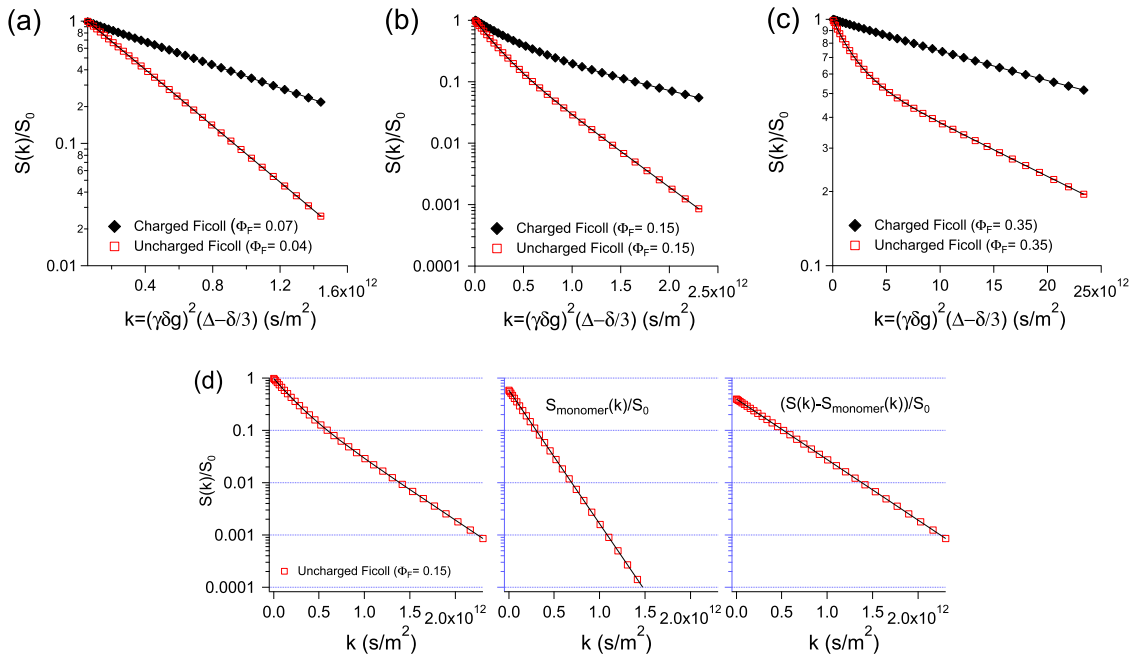


FIG. 2. (a) The attenuation of the signal $S(k)/S(0)$ on a log scale versus the gradient strength parameter $k = (\gamma\delta g)^2(\Delta - \delta/3)$ (s/m^2) for an aqueous solution Ficoll70 is mono-exponential at low Φ_F for both uncharged and charged Ficoll70 solutions. (b) For $\Phi_F > 0.05$ (0.10) for uncharged (charged) Ficoll70, the signal attenuation is not mono-exponential. As an example, signal attenuation for the Ficoll70 solution at $\Phi_F = 0.15$ and (c) at $\Phi_F = 0.35$, is well-fit to a bi-exponential form. (d) Signal attenuation for the uncharged Ficoll70 solution at $\Phi_F = 0.15$ is shown alongside decoupled monomer and cluster signal attenuations obtained after the bi-exponential fit.

On the other hand, if the molecular exchange between the monomer and cluster is very slow, one expects the total Ficoll70 signal to be given by

$$\begin{aligned} S(k) &= S_{\text{monomer}}(k) + S_{\text{cluster}}(k) \\ &= S_{\text{monomer}}(0) \exp(-D_{\text{monomer}}k) \\ &\quad + S_{\text{cluster}}(0) \exp(-D_{\text{cluster}}k) \end{aligned} \quad (3)$$

which is bi-exponential in nature [Figs. 2(b) and 2(c)]. A generalization to multi-exponential behaviour may be made for macromolecules existing in more than two species: $S(k) = \sum_i S_i(k)$, where $i = \text{monomer or cluster}$. For two species, Eq. (3) may be written in the form $S(k)/S(0) = f \exp(-D_{\text{monomer}}k) + (1-f) \exp(-D_{\text{cluster}}k)$, where $f = S_{\text{monomer}}(0)/(S_{\text{monomer}}(0) + S_{\text{cluster}}(0))$.

IV. RESULTS

A. Ficoll70 forms clusters

The self-diffusion coefficient is obtained in pure Ficoll70 aqueous solutions. The key observation is that the PFG NMR signal attenuation is not mono-exponential when Φ_F is greater than a threshold value: 0.05 (0.10) for uncharged (charged) Ficoll70. When there are two species with the same chemical signatures, and when there is a slow exchange (or no exchange) between the species, one obtains bi-exponential signal attenuations in a PFG NMR experiment [Figs. 2(b) and 2(c)]. Shown in the [supplementary material](#) is a plot of the coefficient of determination R^2 in a linear fit of $\log(S(k))$ vs. k . For $\Phi_F = 0.05$ and greater, there is a marked decrease in R^2 below a plateau value of 0.99. This signals the onset of

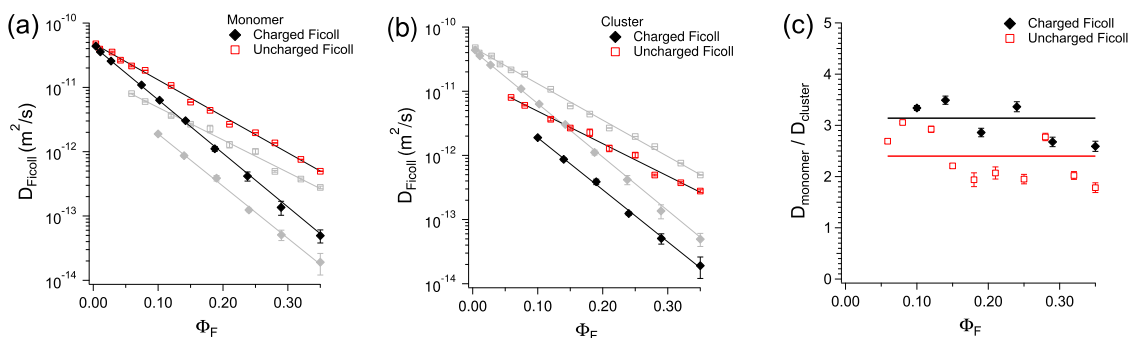


FIG. 3. Ficoll70 forms clusters: Biexponential signal attenuation indicates emergence of a cluster state above $\Phi_F = 0.05$ (uncharged) and $\Phi_F = 0.1$ (charged). (a) Ficoll70 monomer diffusion coefficient as a function of Φ_F and (b) Ficoll70 cluster diffusion coefficient as a function of Φ_F . (c) The monomer-to-cluster self-diffusivity ratio shows no clear dependence on Φ_F but appears somewhat larger for charged Ficoll70 than for uncharged Ficoll70. In (a) and (b), the cluster results are shown in gray to aid comparison.

cluster formation. Our observations thus indicate the co-existence of (fast diffusing) monomers and (slow diffusing) clusters of Ficoll70.

We plot the diffusion coefficients for charged and uncharged crowder, and for monomer [Fig. 3(a)] and for cluster [Fig. 3(b)], as a function of Φ_F . Every D dependence on Φ_F is exponential! In dilute polymer solutions one sees a linear decrease in diffusivity. The corresponding diffusion interaction parameter k_D is ~ -2.3 for polystyrene solutions when the second virial coefficient A_2 is zero.³⁸ A_2 is negative for lower (more negative) k_D . For hard-sphere colloids, the linear Φ_F term would have a prefactor of ~ -2.5 . A linearization of the exponential dependence that we observe yields $k_D \sim -9.5$ (-10.4) for uncharged (charged) Ficoll70, much larger than those for typical polymer solutions or hard-sphere colloids, possibly indicative of the propensity for Ficoll to self-associate.

As discussed in earlier¹ and companion²⁶ works, the work of Rosenfeld³⁹ and Dzugutov⁴⁰ connected structural properties of atomic liquids to their diffusion coefficients. Both studies have proposed an exponential relationship between atomic diffusion and the excess entropy S_2/k_B (in the 2-particle approximation); moreover, recent 2D simulations and colloids experiments⁴¹ show that S_2/k_B is proportional to the colloid packing fraction for packing fractions less than 0.4. The same connection would hold in colloidal suspensions if hydrodynamics is not important in the long-time limit.

The spectral selectivity of PFG NMR allows us to simultaneously obtain diffusion coefficients of water and Ficoll70. We can thus obtain not only Ficoll70 dynamics but also the information about the interaction of water with the crowder.

The monomer-to-cluster self-diffusivity ratio [Fig. 3(c)] shows no clear dependence on Φ_F but appears somewhat larger for charged Ficoll70 than for uncharged Ficoll70. When the Stokes-Einstein relation remains valid (i.e., at low enough Φ_F), this ratio should report on the ratio of cluster to monomer sizes. This ratio is approximately 2.5 and 3, respectively, for uncharged and charged Ficoll70. For uncharged Ficoll70, Georgalis *et al.* have measured the value of $D_{\text{monomer}}/D_{\text{cluster}} = 2.37$,²⁵ which is consistent with this work. The fraction of clusters (shown in Fig. 4) increases from 5% at onset of clustering to $\sim 60\%$ in the crowding regime: in fact, this fraction is very similar for charged and uncharged crowder.

The clusters reported here are unlike micellar aggregates in that the cluster sizes are tiny (2-3 as opposed to an aggregation number of 50-80 in micelles) and are more similar to the equilibrium clusters seen in protein solutions and in colloids with competing attractive and repulsive interactions.^{28,29} As an additional note, one would expect there to be a distribution of cluster sizes. However, we cannot obtain fit to a distribution without adding an additional fit parameter. The cluster size should thus be treated as a mean cluster size.

One can use the measured monomer and cluster self-diffusivities to calculate an effective diffusion coefficient D_{eff} ,

$$D_{\text{Ficoll}}^{\text{eff}} = f_{\text{cluster}} D_{\text{cluster}} + (1 - f_{\text{cluster}}) D_{\text{monomer}}. \quad (4)$$

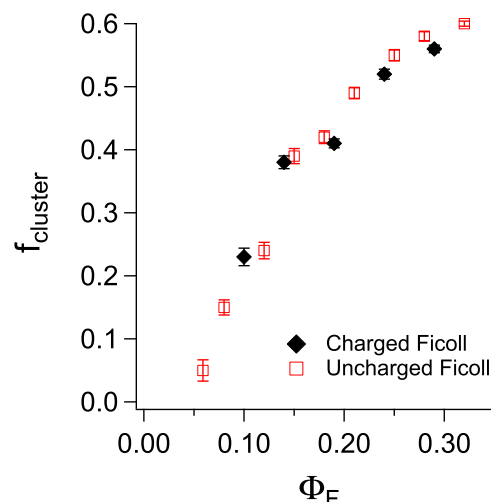


FIG. 4. Structure of Ficoll70 via diffusion: Fraction of Ficoll70 cluster (f_{cluster}) as a function of Φ_F for both charged and uncharged Ficoll70.

This diffusivity may be compared to its bulk analog from the measured bulk Ficoll70 viscosity η_{Bulk} and the hydrodynamic radius of Ficoll70 monomer $R_H = 4.6$ nm using a Stokes-Einstein form $k_B T / (6\pi\eta_{\text{Bulk}}R_H)$. A slope of 1 in the plot of $k_B T / (6\pi\eta_{\text{Bulk}}R_H)$ versus D_{eff} would imply agreement with the Stokes-Einstein behaviour (dashed line). As can be seen in Fig. 5, there is agreement for uncharged Ficoll70 solutions so long as cluster formation is not significant, while for charged Ficoll70, there is significant deviation for much smaller Φ_F than the cluster-forming threshold. Even for uncharged Ficoll70 solutions, there is significant deviation for $\Phi_F > 0.15$.

B. Ficoll hydration is quantifiable via water dynamics

Another interesting aspect is the water diffusion coefficient. The similarity of the water diffusion for charged and uncharged Ficoll70 in Fig. 6 is reassuring, as it indicates that

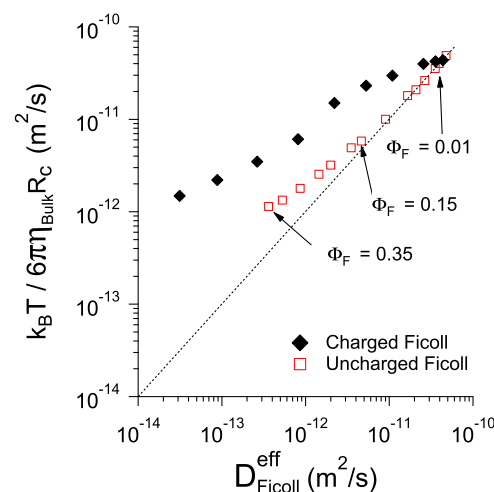


FIG. 5. Effective diffusion coefficient of Ficoll70: Comparison of a self-diffusivity $k_B T / (6\pi\eta_{\text{Bulk}}R_c)$, calculated from the bulk Ficoll70 viscosity η_{Bulk} and the mean radius of the Ficoll70 monomer $R_c = 4.6$ nm, as a function of the measured effective diffusion coefficient D_{eff} , shows agreement with the Stokes-Einstein behaviour (dashed line) upto $\Phi_F = 0.15$ for uncharged Ficoll70, while for charged Ficoll70 there is significant deviation for much smaller Φ_F .

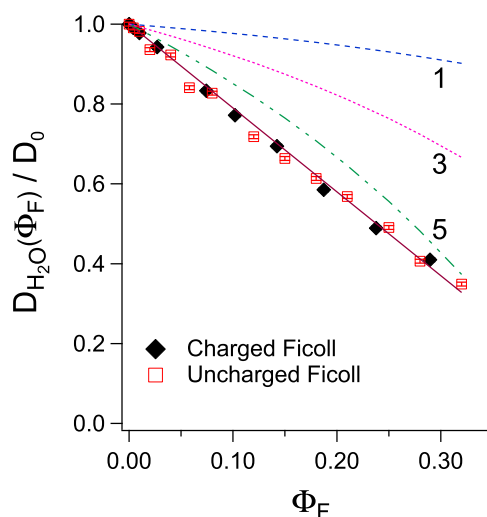


FIG. 6. Ficoll70 hydration: Linear decrease in the water diffusion coefficient with increasing Φ_F indicates a linear increase in the fraction of surface-associated water. The slope is a useful quantifier of Ficoll70 hydration. The dashed curves show that the expectation for n water layers ($n = 1, 3, 5$) on the surface of a solid is nonlinear.

the physical structure of the polysucrose is unchanged by the charge.

Why does the water diffusion coefficient change with Φ_F ? Water dynamics, measured on PFG NMR time scales, is well modeled by assuming rapid exchange of the water molecule between bulk and surface-associated environments.⁴² In the present case, the self-diffusion of the surface-associated water would be similar to that of the Ficoll70 particle, i.e., between 20 and 1000 times slower than that of the bulk water self-diffusion coefficient. In the rapid exchange limit, the observed diffusion coefficient $D_{H_2O}(\Phi_F) = f D_0 + (1 - f)D_{\text{surface}}$, where f is the fraction of free (bulk) water, while $(1 - f)$ is the fraction of surface-associated water. Since $D_{\text{surface}} \ll D_0$, this yields the approximate form for the fraction of free (bulk) water $f \approx D_{H_2O}(\Phi_F)/D_0$; this fraction is shown in Fig. 6.

For solid, spherical colloids, the fraction f of bulk water would be expected to decrease with Φ_F . One water layer is approximately 0.3 nm thick and the Ficoll radius is 4.6 nm. The dependence of $f \equiv D_{H_2O}(\Phi_F)/D_0$ for $n = 1, 3$, and 5 water layers is shown. In contrast, the measured dependence of f on Φ_F (Fig. 6) shows a high degree of linearity, with a fit to $D_{H_2O}/D_0 = 1 - \beta_1 \Phi_F$, with $\beta_1 = 2.10 \pm 0.03$. As shown in the [supplementary material](#) (Sec. IV), $\beta \sim 2$ implies that a water volume per gram of Ficoll70 that corresponds roughly to $2\bar{v}$ (i.e., twice the partial specific volume of Ficoll70) is surface-associated.

At $\Phi_F = 0.3$, as much as 60% of the water is surface associated, suggesting that Ficoll70 is very porous and hydrated; this is not surprising, in hindsight, but we believe that it has not been adequately recognized in the crowding literature, apart from clear indications that Ficoll70 is not a rigid sphere,^{5,6} as well as the practical knowledge about the lack of overall stability of Ficoll70 solutions above $\Phi_F = 0.35$. It should be noted that this bound water is likely not available to the polymer and should be accounted for in any free-volume calculations.

V. DISCUSSION AND CONCLUSION

In this work, we examine the dynamics of Ficoll70 in water, for both uncharged and charged system. Ficoll70, an often-used artificial crowder, is not hard-sphere-like. This has been indicated elsewhere,^{5,6} but our water diffusion measurements suggest that 60% of the water is surface-associated in the crowding limit, indicating that the polysucrose particle is highly porous. Even more surprisingly, Ficoll70 diffusivity is bi-modal, indicating that it self-clusters at modest concentrations, with cluster sizes approaching 2–3 times the size of the single Ficoll70 particle size (“monomer”). This is reminiscent of indications, from maximum entropy analyses of fluorescence correlation spectroscopy experiments, of multiple modes of probe mobility in crowded solutions.⁴³

Coexistence of monomers and clusters in equilibrium has been seen experimentally^{28–30} and is expected in systems which have short-ranged attractions and longer-ranged repulsions.^{27,32} Considering both the 5 nm particle scale and that polysaccharide surfaces in water have a Hamaker constant of $\sim 2k_B T^{44}$, attractive forces should be relevant in the presence of even small long-ranged (e.g. electrostatic) repulsions and is consistent with the observed weak clustering.

The generic behavior—formation of small clusters with the fraction of clusters increasing with packing fraction Φ_F and the exponential dependence of all the self-diffusivities as a function of Φ_F —is the same for uncharged and charged Ficoll70 solutions. The striking difference is in the actual values of the self-diffusivities, with the charged Ficoll70 being as much as an order of magnitude slower in the crowding limit. A more detailed understanding of the Ficoll70 structure and inter-particle interactions will be necessary in order to understand this difference.

SUPPLEMENTARY MATERIAL

See [supplementary material](#) for results on bulk viscosity measurements for aqueous solutions of charged and uncharged Ficoll70, a plot of the coefficient of determination that exhibits the method to determine the transition region between mono and bi-exponential fit, the effective diffusion coefficient using a “two-species model” for charged and uncharged Ficoll70, and a calculation that examines alternative models for the expected dependencies of the water diffusion coefficient on volume fraction.

ACKNOWLEDGMENTS

This work was supported by the Natural Sciences and Engineering Research Council of Canada. We thank William Fissell for generously providing us with charged Ficoll70 and Arun Yethiraj and Francesco Piazza for illuminating discussions.

¹S. Palit, L. He, W. A. Hamilton, A. Yethiraj, and A. Yethiraj, *Phys. Rev. Lett.* **118**, 097801 (2017).

²Y. Wang, M. Sarkar, A. E. Smith, A. S. Krois, and G. J. Pielak, *J. Am. Chem. Soc.* **134**, 16614 (2012).

³K. H. Wong, R. D. Sandlin, T. R. Carey, K. L. Miller, A. T. Shank, R. Oklu, S. Maheswaran, D. A. Haber, D. Irimia, S. L. Stott *et al.*, *Sci. Rep.* **6**, 21023 (2016).

- ⁴J. Groszek, L. Li, N. Ferrell, R. Smith, C. A. Zorman, C. L. Hofmann, S. Roy, and W. H. Fissell, *Am. J. Physiol.: Renal Physiol.* **299**, F752 (2010).
- ⁵W. H. Fissell, S. Manley, A. Dubnisheva, J. Glass, J. Magistrelli, A. N. Eldridge, A. J. Fleischman, A. L. Zydny, and S. Roy, *Am. J. Physiol.: Renal Physiol.* **293**, F1209 (2007).
- ⁶D. Venturoli and B. Rippe, *Am. J. Physiol.: Renal Physiol.* **288**, F605 (2005).
- ⁷A. Dhar, A. Samiotakis, S. Ebbinghaus, L. Nienhaus, D. Homouz, M. Gruebele, and M. S. Cheung, *Proc. Natl. Acad. Sci. U. S. A.* **107**, 17584 (2010).
- ⁸J. R. Wenner and V. A. Bloomfield, *Biophys. J.* **77**, 3234–3241 (1999).
- ⁹A. Galan, B. Sot, O. Llorca, J. L. Carrascosa, J. Valpuesta, and A. Muga, *J. Biol. Chem.* **276**, 957 (2001).
- ¹⁰P. N. Lavrenko, O. I. Mikriukova, and O. V. Okatova, *Anal. Biochem.* **166**, 287 (1987).
- ¹¹N. Tokuriki, M. Kinjo, S. Negi, M. Hoshino, Y. Goto, I. Urabe, and T. Yomo, *Protein Sci.* **13**, 125 (2004).
- ¹²Y. Wang, L. A. Benton, V. Singh, and G. J. Pielak, *J. Phys. Chem. Lett.* **3**, 2703 (2012).
- ¹³S. B. Zimmerman and A. P. Minton, *Annu. Rev. Biophys. Biomol. Struct.* **22**, 27 (1993).
- ¹⁴M. Bohrer, G. D. Patterson, and P. Carroll, *Macromolecules* **17**, 1170 (1984).
- ¹⁵W. Deen, M. Bohrer, and N. Epstein, *AIChE J.* **27**, 952 (1981).
- ¹⁶J. D. Oliver, S. Anderson, J. L. Troy, B. M. Brenner, and W. Deen, *J. Am. Soc. Nephrol.* **3**, 214 (1992).
- ¹⁷J. Axelsson, K. Sverrisson, A. Rippe, W. Fissell, and B. Rippe, *Am. J. Physiol.: Renal Physiol.* **301**, F708 (2011).
- ¹⁸D. Asgeirsson, D. Venturoli, E. Fries, B. Rippe, and C. Rippe, *Acta Physiol.* **191**, 237 (2007).
- ¹⁹C. Rippe, D. Asgeirsson, D. Venturoli, A. Rippe, and B. Rippe, *Kidney Int.* **69**, 1326 (2006).
- ²⁰M. Ohlson, J. Sörensson, and B. Haraldsson, *Am. J. Physiol.: Renal Physiol.* **279**, F84 (2000).
- ²¹D. Asgeirsson, D. Venturoli, B. Rippe, and C. Rippe, *Am. J. Physiol.: Renal Physiol.* **291**, F1083 (2006).
- ²²C. M. Öberg and B. Rippe, *Am. J. Physiol.: Renal Physiol.* **306**, F844 (2014).
- ²³W. H. Fissell, C. L. Hofmann, R. Smith, and M. H. Chen, *Am. J. Physiol.: Renal Physiol.* **298**, F205 (2010).
- ²⁴P. Lavrenko, O. Mikryukova, and S. Didenko, *Polym. Sci. U.S.S.R.* **28**, 576 (1986).
- ²⁵Y. Georgalis, M. Philipp, R. Aleksandrova, and J. Krüger, *J. Colloid Interface Sci.* **386**, 141 (2012).
- ²⁶S. Palit, L. He, W. A. Hamilton, A. Yethiraj, and A. Yethiraj, “The effect of crowder charge in a model polymer–colloid system for macromolecular crowding: polymer structure and dynamics,” *J. Chem. Phys.* (submitted).
- ²⁷J. Groenewold and W. K. Kegel, *J. Phys. Chem. B* **105**, 11702 (2001).
- ²⁸A. Stradner, H. Sedgwick, F. Cardinaux, W. Poon, S. Egelhaaf, and P. Schurtenberger, *Nature* **432**, 492 (2004).
- ²⁹S. Barhoum and A. Yethiraj, *J. Phys. Chem. B* **114**, 17062 (2010).
- ³⁰L. Porcar, P. Falus, W.-R. Chen, A. Faraone, E. Fratini, K. Hong, P. Baglioni, and Y. Liu, *J. Phys. Chem. Lett.* **1**, 126 (2010).
- ³¹S. Barhoum, A. Agarwal, and A. Yethiraj, in *New Challenges in Electrostatics of Soft and Disordered Matter*, edited by D. Dean, J. Dobnikar, A. Naji, and R. Podgornik (Pan Stanford, 2013).
- ³²M. B. Sweatman, R. Fartaria, and L. Lue, *J. Chem. Phys.* **140**, 124508 (2014).
- ³³J. Sörensson, M. Ohlson, K. Lindström, and B. Haraldsson, *Acta Physiol. Scand.* **163**, 83 (1998).
- ³⁴C. Le Coeur, “Influence de l’encombrement cytoplasmique sur la stabilité et la diffusion des protéines,” Ph.D. thesis, L’Université Pierre et Marie Curie, 2010.
- ³⁵K. Luby-Phelps, P. E. Castle, D. L. Taylor, and F. Lanni, *Proc. Natl. Acad. Sci. U. S. A.* **84**, 4910 (1987).
- ³⁶W. S. Price, *Concepts Magn. Reson.* **9**, 299 (1997).
- ³⁷S. Barhoum, S. Palit, and A. Yethiraj, *Prog. Nucl. Magn. Reson. Spectrosc.* **94-95**, 1 (2016).
- ³⁸C. C. Han and Z. A. Akcasu, *Scattering and Dynamics of Polymers* (Wiley, Singapore, 2011).
- ³⁹Y. Rosenfeld, *Phys. Rev. A* **15**, 2545 (1977).
- ⁴⁰M. Dzugutov, *Nature* **381**, 137 (1996).
- ⁴¹A. L. Thorneywork, R. E. Rozas, R. P. A. Dullens, and J. Horbach, *Phys. Rev. Lett.* **115**, 268301 (2015).
- ⁴²A. Yethiraj, D. Capitani, N. E. Burlinson, and E. E. Burnell, *Langmuir* **21**, 3311 (2005).
- ⁴³A. B. Goins, H. Sanabria, and M. N. Waxham, *Biophys. J.* **95**, 5362 (2008).
- ⁴⁴M. Holmberg, J. Berg, S. Stemme, L. Öberg, J. Rasmusson, and P. Claesson, *J. Colloid Interface Sci.* **186**, 369 (1997).